Human Genetics (2019) 138:1259–1266
https://doi.org/10.1007/s00439-019-02065-x

ORIGINAL INVESTIGATION

Biallelic variants in *AGMO* with diminished enzyme activity are associated with a neurodevelopmental disorder

Volkan Okur[1] · Katrin Watschinger[2] · Dmitriy Niyazov[3] · Julie McCarrier[4] · Donald Basel[4] · Martin Hermann[5] · Ernst R. Werner[2] · Wendy K. Chung[1,6]

Received: 9 July 2019 / Accepted: 15 September 2019 / Published online: 25 September 2019

Abstract

Alkylglycerol monooxygenase (AGMO) is the only enzyme known to cleave the *O*-alkyl bonds of ether lipids (alkylglycerols) which are essential components of cell membranes. A homozygous frameshift variant [p.(Glu324LysfsTer12)] in *AGMO* has recently been reported in two male siblings with syndromic microcephaly. In this study, we identified rare nonsense, in frame deletion, and missense biallelic variants in *AGMO* in two unrelated individuals with neurodevelopmental disabilities. We assessed the activity of seven disease associated *AGMO* variants including the four variants identified in our two affected individuals expressed in human embryonic kidney (HEK293T) cells. We demonstrated significantly diminished enzyme activity for all disease-associated variants, supporting the mechanism as decreased AGMO activity. Future mechanistic studies are necessary to understand how decreased AGMO activity leads to the neurologic manifestations.

Introduction

Alkylglycerol monooxygenase (AGMO; EC 1.14.16.5) is the only enzyme known to cleave the *O*-alkyl bonds of ether lipids (alkylglycerols), which are essential components of cell membranes. The reaction is tetrahydrobiopterin dependent and yields glycerol and aldehyde. Glycerol is a precursor for triacylglycerols and phospholipids as well as an energy source, and aldehyde is detoxified by fatty aldehyde dehydrogenase (ALDH3A2) (Watschinger et al. 2010). The enzyme is encoded by a 14-exon gene (*AGMO*; also known as *TMEM195*) that maps to 7p21.2 and is highly expressed in liver as well as in testis and small intestine (Consortium G 2015). It is localized to the endoplasmic reticulum and predicted to have nine transmembrane and one membrane associated domains (Watschinger and Werner 2013). It contains a fatty acid hydroxylase motif that consists of eight conserved histidine residues that are predicted to bind iron atoms in a catalytic di-iron center (Fig. 1).

A homozygous frameshift variant [p.(Glu324LysfsTer12)] in *AGMO* (#MIM 613738) has recently been reported in two siblings with syndromic microcephaly (Alrayes et al. 2016). *AGMO* has also been reported to have a role in visceral leishmaniasis (Kala-azar) relapse via its role in

Volkan Okur and Katrin Watschinger contributed equally to this work.

Ernst R. Werner and Wendy K. Chung contributed equally to this work.

Electronic supplementary material The online version of this article (https://doi.org/10.1007/s00439-019-02065-x) contains supplementary material, which is available to authorized users.

✉ Ernst R. Werner
ernst.r.werner@i-med.ac.at

✉ Wendy K. Chung
wkc15@columbia.edu

[1] Department of Pediatrics, Columbia University Medical Center, 1150 St. Nicholas Avenue, New York, NY 10032, USA

[2] Institute of Biological Chemistry, Biocenter, Center for Chemistry and Biomedicine (CCB), Medical University of Innsbruck, 6020 Innsbruck, Austria

[3] Department of Pediatrics, Ochsner Clinic, New Orleans, LA 70394, USA

[4] Department of Pediatrics, Medical College of Wisconsin, Milwaukee, WI 53226, USA

[5] Department of Anesthesiology and Critical Care Medicine, Medical University of Innsbruck, 6020 Innsbruck, Austria

[6] Department of Medicine, Columbia University Medical Center, New York, NY 10032, USA

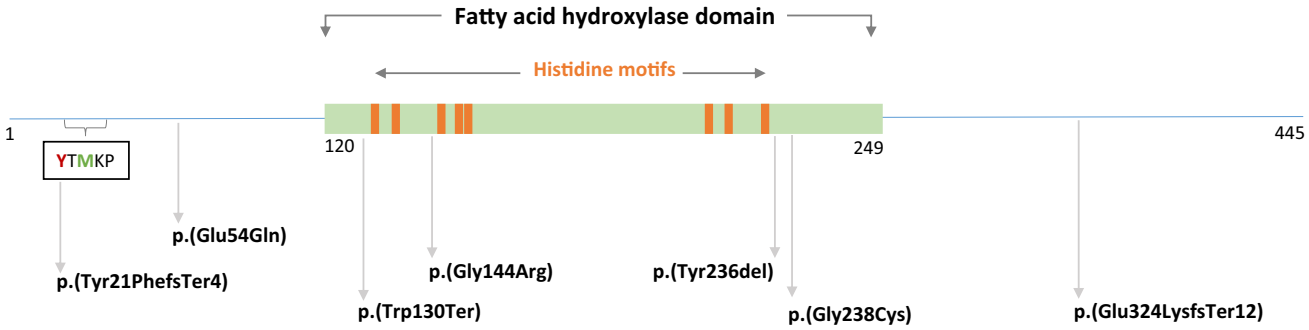

Fig. 1 2D schematic of AGMO protein. The 5-amino acid long sequence box on the left shows the mutated Tyr21 residue (red) and the putative alternative initiation codon (Met23; green). Fatty acid hydroxylase domain is shown in green and histidine residues (His132, His136, His145, His148, His149, His221, His224, His235) that are crucial for active site are shown in orange

macrophage-mediated immunity (Marquet et al. 2017). Here, we report two unrelated individuals with neurodevelopmental disabilities with biallelic rare, predicted deleterious variants in *AGMO* and provide functional data about the AGMO catalytic activity of the variants.

Materials and methods

Ascertainment of the individuals

This study was approved by the institutional review board at Columbia University. Clinical data and DNA samples were collected from the participating families after written informed consent was obtained. Clinical exome and genome sequencing along with Sanger sequencing of the identified variants have been performed on peripheral blood samples of available family members.

Recombinant expression of *AGMO* variants

Untagged human AGMO cDNA in pCMV-Sport6 was from the Mammalian Gene Collection (Accession BC108676). N-terminally 6xmyc tagged human AGMO was introduced into pEXPR-Iba5 (Iba, Göttingen, Germany) by standard cloning techniques. Variants were introduced by the QuikChange II Site-Directed Mutagenesis Kit (Agilent, Vienna, Austria) and verified by sequencing. HEK293T cells (obtained from ATCC via LGC Standards, Wesel, Germany) were transfected with untagged or N-terminally 6xmyc tagged AGMO as indicated in the individual figures together with fatty aldehyde dehydrogenase [ALDH3A2; NM_000382 subcloned in pcDNA3.1(+)] with TurboFect (Thermo Scientific, Vienna, Austria) using a total of 8 µg DNA per transfection (Table S1). For co-expression experiments we kept the total amount of 8 µg DNA constant and reduced each component from 4 to 2.7 µg accordingly. In case of testing the effect of plasmid combinations, we added single plasmids twice to ensure a constant DNA amount for transfection, and indicated this by listing the plasmids with the double concentration twice in Table S2. After 48 h cultivation in presence or absence of tetrahydrobiopterin precursor sepiapterin (SP, 1 µM in medium, Schircks, Jona, Switzerland) cells were harvested in 0.5% CHAPS and 1 mM dithioerythritol and snap frozen in liquid nitrogen. AGMO activity was determined by an assay modified from (Werner et al. 2007). Cellular homogenates were incubated with 1-*O*-pyrenedecyl-sn-glycerol (Otava, Vaughan, Ontario, Canada) as substrate in the presence of 200 µM 6R-tetrahydro-L-biopterin (Schircks, Jona, Switzerland) and 25 µg/ml recombinant fatty aldehyde dehydrogenase (Keller et al. 2014). AGMO activity was quantified by the amount of pyrenedecanoic acid formed as measured by reversed-phase HPLC with fluorescence detection.

Western blotting

AGMO was stained with anti-AGMO (anti-TMEM195) rabbit polyclonal antibody (dilution 1:1000; Proteintech, Manchester, UK) and the 6× myc tag was detected with rabbit polyclonal anti c-myc (A-14) antibody (dilution 1:1000; Santa Cruz Biotechnology, Inc.). As a secondary antibody we used goat anti-rabbit CyTM5 (1:2500; GE Healthcare, Vienna, Austria). Actin was used as visual loading control and stained with mouse anti-actin antibody (dilution, 1:1500; Millipore, Vienna, Austria) and goat anti-mouse CyTM3 (1:1250; GE Healthcare). Blots were scanned using a red laser (633 nm excitation and 670 nm emission; BP30) for Cy5 and a green laser (532 nm excitation and 580 nm emission; BP30) for Cy3 with a Typhoon 9410 (GE Healthcare). Blot signals were quantified by ImageQuant TL software (GE Healthcare) and divided by the respective amount of protein applied to the gel (12.5–30 µg). Statistical analysis was performed with GraphPad Prism 7.03, using 1-way analysis of variance, followed by the Tukey multiple comparisons test.

Real time live confocal microscopy

HEK293T cells were seeded in a concentration of 4×10^4 cells/well in 8-well µ-slides (Ibidi, Munich, Germany) and transfected with TurboFect using a total of 0.12 µg DNA per transfection. Real time confocal imaging was performed 24 h after transfection with a spinning disk confocal system (UltraVIEW VoX; Perkin Elmer, Waltham, MA, USA) connected to a Zeiss AxioObserver Z1 microscope (Zeiss, Oberkochen, Germany). GFP-constructs were excited with a wavelength of 488 nm. Images were acquired with the Volocity software (Perkin Elmer) using a 40× water immersion objective with a numerical aperture of 1.2.

Results

Clinical data

Clinical findings of the two individuals with biallelic *AGMO* variants are summarized in Table 1 and compared to the previously reported two siblings with homozygous *AGMO* frameshift variants.

Individual 1 is an 8-year-old female born at 39 weeks of gestation following a pregnancy complicated with oligohydramnios, maternal hypothyroidism, and decreased fetal movement. Her birth weight was 2892 g (23%) and length was 49.5 cm (50%). Head circumference was not known but noted to be 5–10%. She had mild neonatal jaundice and weak cry. She started having generalized tonic–clonic seizures at 2 months of age characterized by eye fluttering, twitching of the face, hypertonic extension of the extremities, and decreased responsiveness. Seizures were refractory to clonazepam, lorazepam, levetiracetam, valproic acid, intravenous midazolam, propofol, pentobarbital, and lacosamide. Seizures resolved with the initiation of intravenous fosphenytoin and subsequent maintenance of oral phenytoin. The patient has remained clinically seizure-free on phenytoin monotherapy since 22 months old. She crawled at 12–13 months old and stood with support at 18 months old. The patient lost all motor and cognitive skills after a status epilepticus episode at 18 months of age following an abrupt discontinuation of carbamazepine due to Stevens–Johnson syndrome and transition to clonazepam. At 24 months old, she was significantly below average in all areas with cognitive skills at an 8–10 month old developmental level and aspects of language/communication at a 14-month-old developmental level.

At 7 years and 8 months old she walks/runs well with no excessive falls, feeds self with her hands, can scribble, has a lot of vocalizations but no discernible words. She continues to make slow progress with no regression.

She had a brain MRI at 3 months old which showed mild prominence of cerebrospinal fluid (CSF) space over the frontal and parietal regions. Brain MRI at 1 year old showed possible bilateral volume loss of the hippocampal formation with thinning of the parahippocampal white matter. Vertebral MRI at 14 months old showed mild syringohydromyelia at the thoracic level and conus medullaris. Repeat brain MRI at 2 years old was normal otherwise a minimal stable prominence of the atria and temporal horns of the lateral ventricles.

Individual's parents are of mixed European ethnicity. There is no history of consanguinity. Her paternal grandmother was reported to have epilepsy episodes occurring during sleep that was diagnosed at age 19.

Individual 2 is a 4-year-old male born at 36 weeks and 6 days via vaginally after an unremarkable and uneventful pregnancy. His birth weight was 2977 g (55%) and length was 53.3 cm (98%). There were no anomalies reported during infancy. He sat unsupported at 5.5 months and started walking at 17 months old. He was speaking in sentences at 18 months old. His parents noted regression in eye contact, social interaction, toilet training, and ability to write his name at age 3.5 years old. He also started showing increased issues with sensitivity and anxiety.

He had frequent infections (otitis media, pneumonia, croup, bronchitis) between 7 months and 2 years of age. He had a surgical repair of an undescended testicle at age 1 year old. He was diagnosed as having a probable autism spectrum disorder. He never had a brain MRI. His parents also reported that he has always had a poor weight gain and had significant sleep issues and fatigue during the day.

At 4 years of age, his weight is 16.1 kg (28%), height 102.2 cm (22%), and head circumference 49 cm (16%). He does not have any major dysmorphic facial features. He is able to speak in full sentences but still shows features of autism spectrum disorder such as inadequate eye contact and interaction, and some repetitive behaviors.

His parents are not consanguineous and of Ashkenazi Jewish ancestry. His 20 months old brother is typically developing. He has a nephew with epilepsy and issues with social interaction. There is no other family member with a history of congenital anomalies or known genetic disorders.

Molecular data

Whole genome trio-sequencing in Individual 1 revealed a maternally inherited stop-gain variant [c.389G>A:p.(Trp130Ter)] in trans with a paternally inherited missense variant [c.712G>T:p.(Gly238Cys)] in *AGMO*. Previous genetic tests including chromosomal microarray analysis, comprehensive (53-gene) epilepsy panel, methylation studies for Prader-Willi/Angelman, MECP2 sequencing with

Table 1 Clinical findings of individuals with biallelic *AGMO* variants

	Individual 1	Individual 2	Alrayes et al. (2016)—I[a]	Alrayes et al. (2016)—II[a]
Age	8-year-old	4-year-old	8-year-old	6-year-old
Gender	Female	Male	Male	Male
Ethnicity	European	Ashkenazi Jewish	Middle Eastern	Middle Eastern
Variants	p.Trp130Ter p.Gly238Cys	p.Gly144Arg p.Tyr236del	p.Glu324LysfsTer12 p.Glu324LysfsTer12	p.Glu324LysfsTer12 p.Glu324LysfsTer12
ID/DD	+	Was normal but started to regress at 3.5-year-old	+	+
Microcephaly	+	−	+	+
Seizures	+	−	−	−
Anthropometric measurements	Birth Wt = 2892 g (23%) Lt = 49.5 cm (50%) OFC = not known (5–10%) 8-year old Wt = 24.9 kg (52%) Ht = 123 cm (32%) OFC = 47.5 cm (< 2%)	Birth Wt = 2977 g (55%) Lt = 53.3 cm (98%) OFC = not known 4-year old Wt = 16.1 kg (28%) Ht = 102 cm (22%) OFC = 49 cm (16%)	Birth Not reported 8-year old Wt = 10.5 kg (< 5%) Ht = 88 cm (< 2%) OFC = 42.2 cm (< 3%)	Birth Not reported 6-year old Wt = 7.9 kg (< 5%) Ht = 74 cm (< 2%) OFC = 40 cm (< 3%)
Age at sitting	9 months	5.5 months	Not reported	Not reported
Age at walking	≈ 15 months	17 months	Not reported	Not achieved
Age at speaking and current speech	Patient has a lot of vocalizations but it is difficult to understand words	18 months	Not reported	Non-verbal
Other	Hypothyroidism Congenital hypotonia Difficulty in swallowing Syringomyelia Kyphosis Scoliosis History of thrombocytosis	Cryptorchidism Frequent infections Autism spectrum disorder Sleep issues Lack of energy during the day Poor weight gain MTHFR C677T homozygous	Short stature Difficulty in swallowing Flat occiput Bilateral 5th finger clinodactyly, short hand and fingers Self-mutilating Subclinical hypothyroidism Micropenis	Short stature Difficulty in swallowing Flat occiput Bilateral 5th finger clinodactyly, short hand and fingers Self-mutilating Subclinical hypothyroidism Micropenis
Brain MRI	At 2-year-old Stable MRI with no intracranial abnormality and minimal stable prominence of the atria and temporal horns of the lateral ventricles	Not performed	Delayed myelination and thinning of the corpus callosum	Not performed
EEG	Normal 24-h video EEG at 5 months old	Not performed	Not reported	Not reported

ID/DD intellectual disability/developmental delay, *Wt* weight, *Lt* length, *OFC* occipitofrontal circumference, *Ht* height

[a]These individuals are siblings and born to first cousin parents

deletion/duplication analysis, and GLUT1 sequencing were negative.

Whole exome trio-sequencing in Individual 2 revealed a maternally inherited missense variant [c.430G>A:p.(Gly144Arg)] in trans with paternally inherited in-frame deletion variant [c.706_708delTAT:p.(Tyr236del)] in *AGMO*. Previous genetic tests including chromosomal microarray and fragile-X repeat analysis were negative.

Sanger sequencing confirmed the variants in individual 2 and the parents. Genomic coordinates, population allele frequencies, and in silico predictions are provided for each variant in Table 2. There were no other candidate variants(s) that could explain the phenotypes of the individuals.

Functional studies

AGMO has not been isolated from human tissues owing to its exceptionally labile nature nor has its 3D structure been experimentally determined (Watschinger et al. 2015). Thus, to assess the effects of our rare genetic variants on

Table 2 Genomic characterization of identified variants in *AGMO* (NM_001004320.1)

Variant	Chr7 coordinates (hg19/hg38)	gnomAD frequency (*n* of heterozygotes/homozygotes)	CADD hg19-v1.4	GERP	SIFT	Polyphen-2
c.430G>A p.(Gly144Arg)	15470713 15431088	3.4e−4 (96/1)	26.4	4.85	D	D
c.712G>T p.Gly238Cys	15430495 15390870	4.7e−4 (130/0)	31	5.33	D	D
c.389G>A p.(Trp130Ter)	15584417 15544792	4.1e−6 (1/0)	46	6.13	–	–
c.706_708delTAT p.(Tyr236del)	15430498 15390873	2.5e−4 (62/0)	19.74	–	–	–
c.969delA p.(Glu324LysfsTer12)	15425178 15385553	7.9e−6 (2/0)	–	–	–	–
c.61_62dupTT p.(Tyr21PhefsTer4)	15601409–15601410 15561783–15561784	4.8e−3 (1374/9)	33	–	–	–
c.160G>C p.(Glu54Gln)	15599863 15560238	1.4e−4 (39/0)	26.8	5.93	D	D

D damaging

AGMO activity, we performed recombinant expression of *AGMO* variants reported in this study and by Alrayes et al. (2016) in human embryonic kidney (HEK293T) cells by introducing the AGMO cDNA into an expression plasmid with CMV promoter as previously described (Watschinger et al. 2012, 2018). We found that the AGMO activity was significantly reduced for all five variants reported in individuals with neurodevelopmental disorders (Fig. 2a). The activity was not significantly increased by the treatment of cells with cofactor tetrahydrobiopterin precursor sepiapterin (Table S1). The loss of enzyme activity for the p.(Tyr236del) variant is consistent with the previous site-directed mutagenesis study in which there was reduced activity when this residue was mutated to alanine (Fig. 1) (Watschinger et al. 2012). Glycine residues at positions 144 and 238 are sometimes replaced by alanine in some species but neither arginine (or another positively charged amino acid) nor cysteine, respectively, are found in any other species at those residues. However, there is one individual in gnomAD who is homozygous for the p.Gly144Arg variant.

To determine if decreased activity was caused by diminished protein amounts, we assessed protein levels in the HEK293T cells by Western blotting using an anti-AGMO antibody which showed normal protein levels for the missense variants (Fig. 2b). Undetectable protein for the p.(Trp130Ter) variant is likely due to lack of the antibody epitope ranging from amino acid residues 132–333. We, therefore, epitope-tagged p.(Trp130Ter) along with p.(Glu324LysfsTer12) with a N-terminal myc tag, measured the enzymatic activities by comparing them to N-terminally myc-tagged AGMO wild type and performed Western blot analysis using an anti-myc antibody (Fig. 2c). Interestingly, protein levels of p.(Trp130Ter) and p.(Glu324LysfsTer12) were 55% and 107% of the wild type levels, respectively, albeit with no enzyme activity in our experimental system.

Additionally, we tested the enzyme activities of a frameshift variant p.(Tyr21PhefsTer4) that is observed in 9 homozygotes in gnomAD and another missense variant p.(Glu54Gln) that we identified *in trans* with p.(Tyr21PhefsTer4) in a patient with epilepsy and intellectual disability. The p.(Tyr21PhefsTer4) variant had 59% ± 21.3% of the wild type enzyme activity. The protein level of p.(Tyr21PhefsTer4) variant was also 49% of the wild type level. This might be explained by a methionine at amino acid position 23 (p.Met23) (Fig. 1) that could be used as an alternative initiation codon since it is embedded in an optimal Kozak sequence of AxxATGA. This is supported by the presence of a slightly smaller protein on Western Blot (Fig. 2b). The p.(Glu54Gln) variant was found to have 13.5% ± 4.8% of the wild type enzyme activity. Co-transfection of both variants in HEK293T cells resulted in ≈ 77% of enzyme activity (Table S2). We then assessed whether p.(Tyr21PhefsTer4) affects subcellular localization of the enzyme and found that the enzyme was normally localized in endoplasmic reticulum (Fig. 3). These results support the hypothesis that p.(Tyr21PhefsTer4) variant does not significantly decrease AGMO activity or quantity.

Discussion

The results of our study demonstrate that the two individuals reported by us and the two siblings reported by Alrayes et al., 2016 all have negligible AGMO enzyme activity. While western blot studies of the variant constructs revealed normal protein levels for the missense variants, the frameshift and stop-gain variants also had at least ~ 50% protein levels

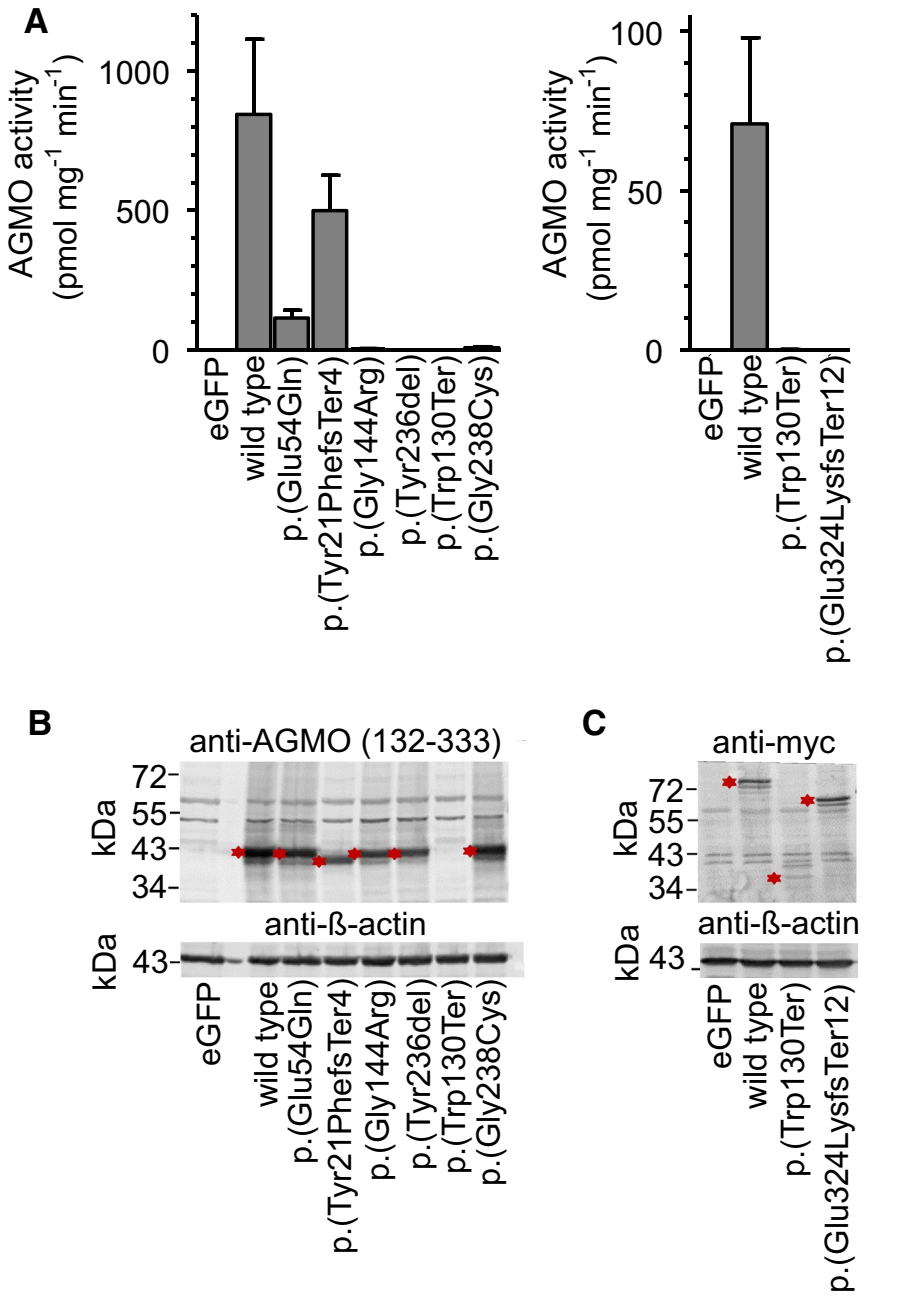

Fig. 2 **a** Enzyme activity levels of *AGMO* variants reported in this study and by Alrayes et al. (2016) compared to wild-type enzyme activity in human embryonic kidney (HEK293T) cells. **b** Western blot results of variant constructs tagged with anti-TMEM195. Anti-TMEM195 antibody was not able to capture the p.(Trp130Ter) construct. **c** N-myc tagged expression studies for p.(Trp130Ter) and p.(Glu324LysfsTer12) constructs, respectively. Stars indicate the bands corresponding to the wild-type and variant constructs

of the wild-type construct. Our artificial expression system in HEK cells does not directly assess the protein expression levels in the patients, and the p.(Tyr130Ter) and p.(Glu324LysfsTer12) variants might actually result in nonsense mediated decay (NMD) in humans. Nevertheless, the active site of the enzyme that has eight essential histidines located downstream of the premature termination at amino acid 130 and significant portion of the carboxy terminus would be lost for p.(Tyr130Ter) and p.(Glu323LysTer12) variants, respectively (Watschinger et al. 2012).

We also found that a relatively common frameshift variant, p.(Tyr21PhefsTer4), retains normal enzyme activity which may explain the presumably unaffected status of 9 homozygotes on gnomAD. Homozygosity of another stop-gain variant [p.(Arg405Ter)] was also recently reported in two otherwise healthy individuals with visceral leishmaniasis relapse (Marquet et al. 2017). By the same methods used in this study, it was previously shown that this variant also has half of the wild type enzyme activity (Watschinger et al. 2018). This variant might escape NMD, as it is located at 51 base pair upstream of the last exon–exon junction, which might explain the lack of neurological phenotype in individuals homozygous for this variant.

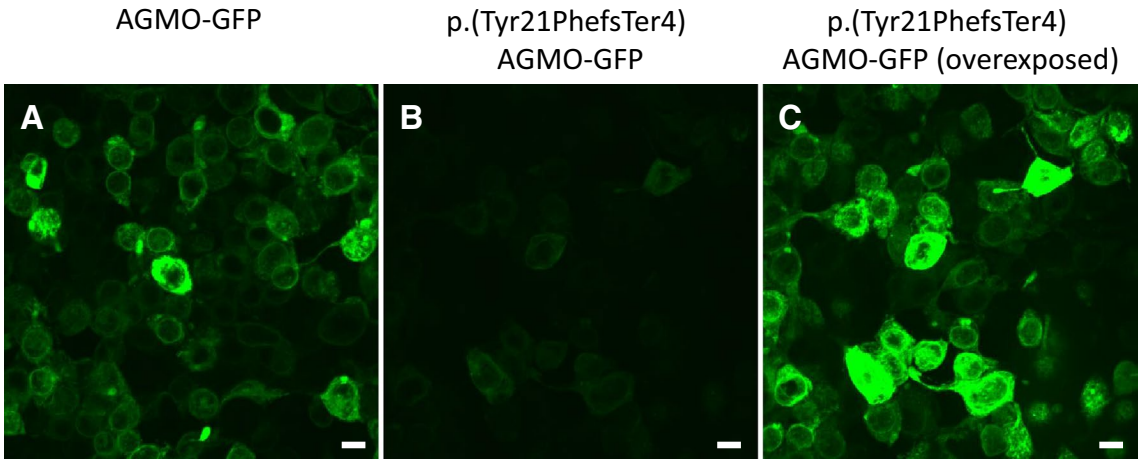

Fig. 3 Real time live confocal imaging of HEK cells transfected with **a** AGMO-GFP and **b** p.(Tyr21PhefsTer4) AGMO-GFP constructs. Note the lower fluorescence intensity of the cells transfected with the p.(Tyr21PhefsTer4) AGMO-GFP construct. **c** For a better visualization of the localization of p.(Tyr21PhefsTer4) AGMO-GFP, the laser intensity was increased. Bar 10 µm

Ether lipids are important components of all cell membranes, particularly in the nervous system, and deficiency in ether lipid biosynthesis due to biallelic pathogenic variants in *PEX7* (MIM #601757) results in rhizomelic chondrodysplasia punctata (MIM #215100) in humans. Ether lipids are also deficient in peroxisomal biogenesis disorders (Dorninger et al. 2017). Alkylglycerol monooxygenase (AGMO) plays an essential role in ether lipid metabolism and is the only known enzyme that breaks down the *O*-alkyl bonds of ether lipids. It has wide substrate specificity, and the final reaction product fatty aldehyde is a toxic metabolite to cells and is immediately degraded by ALDH3A2, deficiency of which is associated with Sjogren-Larsson Syndrome (MIM #270200); an autosomal recessively inherited condition characterized with ichthyosis, intellectual disability, spastic paraparesis, leukoencephalopathy, and macular dystrophy. The phenotype of individuals with biallelic *AGMO* variants does not resemble those syndromes.

There is no knockout mouse model of *Agmo*, but the inhibition of AGMO enzyme activity in murine macrophage cell line RAW264.7 resulted in an accumulation of free alkylglycerols, which in turn fed back into more complex ether lipids, mainly alkyl-acyl- and alkenyl-acyl-phospholipids. Interestingly, there was no change in lyso-PAF levels, a direct substrate of AGMO (Watschinger et al. 2015). Thus, it is yet to be known the exact physiological consequences of loss of AGMO enzyme activity. All patients with deleterious *AGMO* variants have neurodevelopmental disabilities; however, symptoms vary in severity, age of onset, and accompanying health problems. There are no distinguishing dysmorphic features. As more patients are diagnosed, we may be able to delineate the core clinical and biochemical features to aid in the diagnosis of AGMO deficiency.

In conclusion, we report enzymatic activity of 1 frameshift, 1 stop-gain, and 3 missense *AGMO* variants in HEK293 cells which have been observed in 4 individuals with neurodevelopmental manifestations along with one frameshift variant that is seen in presumably healthy individuals in gnomAD and another missense variant. Future clinical and functional studies are needed to elucidate the underlying mechanisms leading to the neurologic manifestations.

Acknowledgements We thank the families for their generous contribution, and Petra Loitzl, Nina Madl, and Rita Holzknecht for expert technical assistance. This work was supported by Grants from Austrian Science Fund (fwf) projects to Katrin Watschinger (P30800) and Ernst R. Werner (P28769), and the SFARI and the JPB Foundation to Wendy K. Chung.

Author contributions VO analyzed the data, drafted and critically reviewed the manuscript. KW analyzed the data, drafted and critically reviewed the manuscript. DN provided with the clinical data, critically reviewed the manuscript. JM provided with the clinical data, critically reviewed the manuscript. DB provided with the clinical data, critically reviewed the manuscript. MH analyzed the data and critically reviewed the manuscript. ERW conceived of the study, analyzed the data, drafted, and critically reviewed the manuscript. WKC conceived of the study, analyzed the data, drafted and critically reviewed the manuscript.

Compliance with ethical standards

Conflict of Interest The authors declare no competing interests related to presented study.

References

Alrayes N, Mohamoud HS, Ahmed S, Almramhi MM, Shuaib TM, Wang J, Al-Aama JY, Everett K, Nasir J, Jelani M (2016) The alkylglycerol monooxygenase (AGMO) gene previously involved

in autism also causes a novel syndromic form of primary microcephaly in a consanguineous Saudi family. J Neurol Sci 363:240–244. https://doi.org/10.1016/j.jns.2016.02.063

Consortium G (2015) Human genomics. The genotype-tissue expression (GTEx) pilot analysis: multitissue gene regulation in humans. Science 348:648–660. https://doi.org/10.1126/science.1262110

Dorninger F, Forss-Petter S, Berger J (2017) From peroxisomal disorders to common neurodegenerative diseases—the role of ether phospholipids in the nervous system. FEBS Lett 591:2761–2788. https://doi.org/10.1002/1873-3468.12788

Keller MA, Zander U, Fuchs JE, Kreutz C, Watschinger K, Mueller T, Golderer G, Liedl KR, Ralser M, Krautler B, Werner ER, Marquez JA (2014) A gatekeeper helix determines the substrate specificity of Sjogren-Larsson Syndrome enzyme fatty aldehyde dehydrogenase. Nat Commun 5:4439. https://doi.org/10.1038/ncomms5439

Marquet S, Bucheton B, Reymond C, Argiro L, El-Safi SH, Kheir MM, Desvignes JP, Beroud C, Mergani A, Hammad A, Dessein AJ (2017) Exome sequencing identifies two variants of the alkylglycerol monooxygenase gene as a cause of relapses in visceral leishmaniasis in children, in Sudan. J Infect Dis 216:22–28. https://doi.org/10.1093/infdis/jix277

Watschinger K, Werner ER (2013) Alkylglycerol monooxygenase. IUBMB Life 65:366–372. https://doi.org/10.1002/iub.1143

Watschinger K, Keller MA, Golderer G, Hermann M, Maglione M, Sarg B, Lindner HH, Hermetter A, Werner-Felmayer G, Konrat R, Hulo N, Werner ER (2010) Identification of the gene encoding alkylglycerol monooxygenase defines a third class of tetrahydrobiopterin-dependent enzymes. Proc Natl Acad Sci USA 107:13672–13677. https://doi.org/10.1073/pnas.1002404107

Watschinger K, Fuchs JE, Yarov-Yarovoy V, Keller MA, Golderer G, Hermetter A, Werner-Felmayer G, Hulo N, Werner ER (2012) Catalytic residues and a predicted structure of tetrahydrobiopterin-dependent alkylglycerol mono-oxygenase. Biochem J 443:279–286. https://doi.org/10.1042/bj20111509

Watschinger K, Keller MA, McNeill E, Alam MT, Lai S, Sailer S, Rauch V, Patel J, Hermetter A, Golderer G, Geley S, Werner-Felmayer G, Plumb RS, Astarita G, Ralser M, Channon KM, Werner ER (2015) Tetrahydrobiopterin and alkylglycerol monooxygenase substantially alter the murine macrophage lipidome. Proc Natl Acad Sci USA 112:2431–2436. https://doi.org/10.1073/pnas.1414887112

Watschinger K, Keller MA, Golderer G, Coassin S, Zschocke J, Werner ER (2018) Biochemical characterization of AGMO variants implicated in relapses in visceral leishmaniasis. J Infect Dis 217:1846–1847. https://doi.org/10.1093/infdis/jiy090

Werner ER, Hermetter A, Prast H, Golderer G, Werner-Felmayer G (2007) Widespread occurrence of glyceryl ether monooxygenase activity in rat tissues detected by a novel assay. J Lipid Res 48:1422–1427. https://doi.org/10.1194/jlr.D600042-JLR200